

CALCULATION OF THE HEAT TRANSFER AND TEMPERATURE ON THE AIRCRAFT ANTI-ICING SURFACE

W. Dong, J. J. Zhu, X. H. Min

School of Mechanical Engineering, Shanghai Jiaotong University, Shanghai 200240, CHINA

Phone: +86-021-34206817, Fax: +86-021-62932242, Email: wdong@sjtu.edu.cn

Keywords: *Anti-icing, Heat transfer, Droplet impingement property, Water film, Energy balance*

Abstract

Ice accretion on the aircraft wings, tails or any other key components may seriously change the aerodynamic characteristics of the aircraft, causing lift decreasing, drag increasing, poorer operating quality, and a hazard of the flying safety. Anti-icing/deicing systems are widely used in aircraft. Anti-icing or deicing systems can prevent ice accretion or remove the ice on the aircraft surface to a certain extent, and consequently ensure the flying safety.

A numerical method of the heat transfer and temperature on the aircraft anti-icing surface is presented. An improved anti-icing model, which taking into account of the coupling effects of water film layer and the air boundary layer, is developed. A water film breaking up analysis method using a stability energy balance theory is introduced for calculating surface wetness factor distribution. The coupling effects of heat transfer and mass transfer are considered in the surface temperature calculation. Based on the modified model, a special program is developed to calculate the surface temperature of the anti-icing airfoil, and the computation results are compared with the experiment results.

1 Introduction

Ice accretions will occur on the exposed components of an aircraft such as the windscreen, the wings, the tail and the engine inlet system when the aircraft enter into clouds which contain super-cooled water droplets. In-flight icing may seriously affect the original aerodynamic characteristics and result in handling difficulties. For aircraft engine, ice

accretions on the inlet components can worsen the air ingestion characteristics. In addition, shedded ice may be sucked into the engine and induces serious accident. In order to reduce the hazards caused by in-flight icing, various methods of ice protection system have been developed. These can be classified in de-icing and anti-icing categories. The anti-icing prevents ice accretion on particular surface either by evaporating or partially evaporating super-cooled water droplets that impinge on the surface. The partially evaporating anti-icing system allows the impinging liquid water run back to the unprotected area and form an tolerable ice layer. Most of aircraft adopt thermal anti-icing system with compressor bleed hot air as heating source. In recent years, many computational models of the ice accretion were developed to improve the design of ice protection systems.

Computational simulation codes of icing have been developed at ONEAR, DAR, NASA et al. These ice accretion simulation codes consist of four basic steps[1]: computation of aerodynamic flow; determination of super-cooled water droplet trajectories and local collection efficiency; thermal balance analysis of the air-water-ice-body system; determination of the shape of the ice accretion. For analysis of evaporating anti-icing systems, the step of icing shape prediction can be eliminated as no ice is allowed to accumulate on the surface of component. Flow field around the body can be obtained by solving Euler or Navier-Stokes equations and the convective heat transfer coefficient on the icing surface can be obtained at the same time. Super-cooled water droplet

trajectories can be tracked using a Lagrangian approach[2,3,4] and subsequently the local collection efficiency on the surface can be calculated. Another approach for determining the mass of water droplets impinging on the surface is Eulerian approach, which solves flow field and the water droplet equation of motion using the same grid and numerical techniques. Bourgault et al.[5] have developed a code using Eulerian approach to calculate water impact loads on complex geometries. Both of Lagrangian approach and Eulerian approach can give satisfied water droplet impingement results. Most ice accretion codes compute the surface temperature and predict the ice growth rate using heat and mass balance model given by Messinger[6]. The heat balance model is important for predicting ice accretion process and ice shape. The physics mechanism for icing problem is not well known and the models are improved continuously in order to solve this complex problem more accurately. Al-Khalil[7] utilizes the breakup of a uniformly thin liquid film into individual streams or rivulets to more accurately describe the physics of runback water. Al-Khalil et al.[8,9]developed the heat transfer and water film models for the runback water in numerical simulation thermal anti-icing system. Yi X[10] modified the thermodynamic icing model and finished numerical simulations of rime, glaze and mixed ice accretion on the airfoil surface. Silva et al. [11,12] developed a thermal model considering coupled and mass transfer effects for anti-icing numerical simulation. Al-Khalil et al. [13] validated transient electrothermal de-icing and anti-icing simulations code LEWICE and steady state hot gas and electrothermal anti-icing simulations code ANTICE by results of an experimental program. Whalen E A et al. [14] investigated the aerodynamics phenomenon of the runback ice accretions using boundary-layer measurements and fluorescent-oil flow visualization.

The present study consists of an improved anti-icing model considering the effect of runback water and the coupling effect of water film layer and the air boundary layer. A water film breaking up analysis method using stability energy balance theory is introduced for

calculating the surface wetness factor distribution, heat transfer coefficient and the surface temperature.

2 Collection efficiency calculation

The Super-cooled water droplet trajectories and local collection efficiency are calculated by Lagrangian approach and the flow velocities around the body are obtained from numerical simulation. The equation of motion for water droplets is formulated with the following assumption: the droplets remain spherical; the droplets do not affect the flow field. The equation is,

$$m_w \frac{d\vec{U}}{dt} = \vec{D} + \vec{P} + \vec{G}_w \quad (1)$$

\vec{D} is the drag force on the droplet, \vec{P} is the pressure difference force, \vec{G}_w is gravity force on the droplet, m_w , \vec{U} and $\frac{d\vec{U}}{dt}$ are its mass, velocity and acceleration. the pressure difference force is small, so it can be ignored.

The drag force \vec{D} is,

$$\vec{D} = C_d \cdot \frac{1}{2} \rho_a |\vec{V} - \vec{U}|^2 \cdot A_w \quad (2)$$

ρ_a and \vec{V} are air density and velocity, A_w is frontal area of the droplet, C_d is the drag coefficient and can be computed using experience equation as follows,

$$\frac{C_d \text{Re}_{wa}}{24} = 1 + 0.197 \text{Re}_{wa}^{0.63} + 2.6 \times 10^{-4} \text{Re}_{wa}^{1.38} \quad (3)$$

Re_{wa} is relative Reynolds number and is defined as,

$$\text{Re}_{wa} = \frac{\rho_a d(\vec{V} - \vec{U})}{\mu_a} \quad (4)$$

d is diameter of the droplet, μ_a is air viscosity.

Local collection efficiency β is defined as the ratio of the area of impingement to the area through which the water passes at some distance upstream of the airfoil.

3 Mass balance and Energy balance model

The anti-icing component surface will form a water film, and the water film will runback due to aerodynamic forces. An improved energy balance and mass balance model is developed. This model treats runback water film layer and the air boundary layer as two related regions, the velocity gradient and enthalpy transport are taken into account shown in Fig.1. The heat conduction of solid wall is also considered.

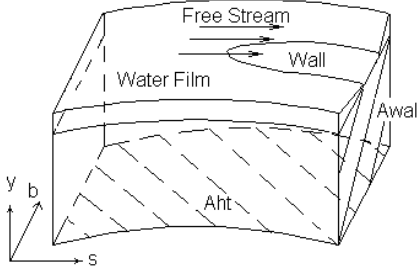


Fig.1 Runback Water Film on the Surface

3.1 Mass balance on the surface

For the control volume, the mass balance equation is,

$$\dot{m}_{in} + \dot{m}_{imp} = \dot{m}_{out} + \dot{m}_{evap} \quad (5)$$

The terms of \dot{m}_{in} , \dot{m}_{imp} , \dot{m}_{out} , \dot{m}_{evap} represent the inlet mass rate, water droplets impingement mass rate, water outlet mass rate and water evaporation mass rate respectively.

Since local collection efficiency has been obtained, the mass flow rate of water droplet impingement can be easily calculated by,

$$\dot{m}_{imp} = \bar{V} \beta A_{ht} \cdot LWC \quad (6)$$

A_{ht} is impingement surface area of the control volume, LWC is the liquid water content.

$$\dot{m}_{evap} = FA_{ht} \frac{0.622Ih_{air}}{c_{p,water}} \left(\frac{p_{v,water} - p_{v,e}}{p_e - p_{v,water}} \right) \quad (7)$$

Where p_v refers to the local saturated vapor pressure, which is a function of temperature; p_e is the local pressure. F is Wetness factor, which was defined as the ratio of wet region area to the total area.

The following volume's inlet face is the current volume's outlet face, and in the stagnation point, there is no mass flow rate through the inlet face, so we can obtain mass flow rate of the each inlet and outlet surface volume by volume.

3.2 Energy balance on the surface

According to the energy conversation law, the energy balance equation can be written as,

$$\begin{aligned} & Q_{anti-ice} + k_{wall} A_{wall} \frac{\partial^2 T}{\partial s^2} + (1-F)r \frac{h_{air} v_e^2}{2c_{p,air}} A_{ht} \\ & = Fh_{water} A_{ht} (T_{wall} - T_{water}) \\ & + (1-F)h_{air} A_{ht} (T_{wall} - T_{rec}) \end{aligned} \quad (8)$$

The terms of the left side of Eq.(8) represent the energy of anti-icing heating, conduction and aerodynamic heating respectively. The terms of the right side of Eq.(8) represent convection heat transfer between wall and water and convection heat transfer between wall and air respectively. Conduction is only considered in s direction, while conduction in y direction is neglected. k_{wall} is thermal conductivity of the solid, c_p is specific heat, r is recovery factor, T_{rec} is the air recovery temperature, T_{rec} can be calculated as follows,

$$T_{rec} = (1-r)T_e + rT_e \left(1 + \frac{k-1}{2} M_e^2 \right) \quad (9)$$

Where k is the ratio of specific heats.

Energy balance equation for the water film can be given as:,

$$\begin{aligned} & Fh_{water} A_{ht} (T_{wall} - T_{water}) + (\dot{m}_{in} c_{p,water} T_{water-in} \\ & - \dot{m}_{out} T_{water-out}) + \dot{m}_{imp} \left[\frac{V_\infty^2}{2} - c_{p,water} (T_{water} - T_\infty) \right] \\ & = Fh_{air} A_{ht} (T_{water} - T_{rec}) + \dot{m}_{evap} [c_{p,water} \cdot \\ & (T_{water} - T_{water-in}) + i] \end{aligned} \quad (10)$$

From left to right, the terms of above equation represent convection heat transfer between water film and wall, the increase of water film's enthalpy, kinetic energy contribution of the impinging droplets, convection heat transfer between water film and air, heat loss by evaporation, respectively. Subscript ∞ represent freestream. $T_{water-in}$ and $T_{water-out}$ are the water temperatures at the inlet and the outlet. i is the latent heat of water. T_{water} is the average temperature of the water film on the surface, which is defined as,

$$T_{water} = \frac{\dot{m}_{in} T_{water-in} + \dot{m}_{out} T_{water-out}}{\dot{m}_{water}} \quad (11)$$

Where \dot{m}_{water} is the average mass of the water film on the surface,

$$\dot{m}_{water} = (\dot{m}_{in} + \dot{m}_{out}) / 2 \quad (12)$$

In the mass and energy equations, convection heat transfer coefficients are needed. They can be approximately got by using the experiential expressions or obtained from the results of CFD computation. For the leading edge, the experienced convection heat transfer coefficient can be calculated using the following equation:

$$Nu_D = \frac{hD}{k} = 1.14 Re_D^{0.5} Pr^{0.4} \left[1 - \left(\frac{\theta}{90} \right)^3 \right] \quad (13)$$

$(\theta \leq 80^\circ)$

D refers to the leading edge's diameter.

Other locations' Nusselt number can be calculated using the following equation,

$$Nu_s = 0.0296 Re_s^{0.8} Pr^{\frac{1}{3}} \quad (14)$$

Where the subscript s refers to the curve length from the stagnation point to the local position.

4 Wetness factor distribution analysis

Surface wetness factor distribution is obtained using stability minimum total energy criteria from the water film breaking up model. The total energy of the runback water film shown in Fig.2 is given as,

$$E_{film-total} = \frac{1}{2} m_{water} \bar{V}_{water}^2 + \sigma_{water-air} l \Delta x + \sigma_{water-wall} l \Delta x + \sigma_{wall-air} (L-l) \Delta x \quad (15)$$

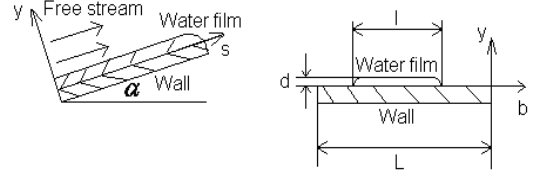


Fig. 2 Water Film Breaking up Model

The terms of the right side of Eq.(15) represent kinetic energy, interfacial energy of water film and air, interfacial energy of water film and wall surface, interfacial energy of air and wall surface respectively.

According to the theory of physical chemistry, the three surface tension coefficients have the following relationship,

$$\sigma_{wall-air} = \sigma_{water-wall} + \sigma_{water-air} \cos \theta_0 \quad (16)$$

Where θ_0 is the static contact angle of water and wall.

$$m_{water} = \rho_{water} l d \Delta x \quad (17)$$

$$\bar{V}_{water}^2 = \frac{1}{y} \int_0^y V_{water}^2 dy \quad (18)$$

Hence, the total energy equation of water film is,

$$E = \frac{m_{water}}{2y} \int_0^y V_{water}^2 dy + \sigma_{water-air} (1 - \cos \theta_0) \frac{m_{water}}{\rho_{water} y} + \sigma_{wall-air} L \Delta x \quad (19)$$

When the film breaks up, there should be,

$$\frac{\partial}{\partial y} E(y) \Big|_{y=d_c} = 0 \quad (20)$$

Assuming the velocity distribution of water film in y direction is liner, the critical thickness and mass flow rate can be obtained as,

$$d_c = 1.442 \left[\frac{\sigma_{water-air} (1 - \cos \theta_0)}{\rho_{water} \left(\frac{\tau}{\mu_{water}} \right)^2} \right]^{1/3} \quad (21)$$

$$\dot{m}_{water,c} = b \rho_{water} \int_0^{d_c} V_{water} dy = 1.04b \cdot \left(\frac{\rho_{water} \mu_{water}}{\tau} \right)^{1/3} \sigma_{water-air}^{2/3} (1 - \cos \theta_0)^{2/3} \quad (22)$$

Where,

$$\tau = \mu_{water} \frac{V_{water,e}}{y} \quad (23)$$

When the mass flow rate of water film is less than the critical mass flow rate, runback water film will break up, and the wetness factor can be calculated as,

$$F = \frac{\dot{m}_{water}}{\dot{m}_{water,c}} \quad (24)$$

Considering water flow is unstable in the impingement region, the wet factors in this region are assumed to be unit.

5 Results and discussion

5.1 Reference case and calculation results

Based on the modified model, a special program is developed to calculate the water droplet impingement characteristics and the surface temperature distributions. One case is chosen to run, and then the obtained surface temperature is compared with the experiment result. The velocity and temperature of freestream is 44.7m/s and -7.6°C, MVD is 20 μm, LWC is 0.78g/m³, attack angle is 0. The sizes of the test airfoil are shown in Fig.3, the power density distributions of the heaters are listed in Table 1 and other test conditions are mentioned in Ref.13.

Fig.4 shows the comparison of local collection efficiency calculated by the program and ONERA2D.

In this case, the heating energy is so large that most of water droplets evaporate as they reach the surface. The wet region falls into the

impinging area and the wet factor is equal to unit.

Table 1 Heaters' Locations and Power Densities

Heater Element	Heater Location (s/c)		Power Density (kW/m ²)
	Start	End	
F	-0.1024	-0.0607	9.92
D	-0.0607	-0.0329	6.98
B	-0.0329	-0.0051	32.5
A	-0.0051	0.0157	46.5
C	0.0157	0.0435	18.6
E	0.0435	0.0713	10.23
G	0.0713	0.1129	10.24

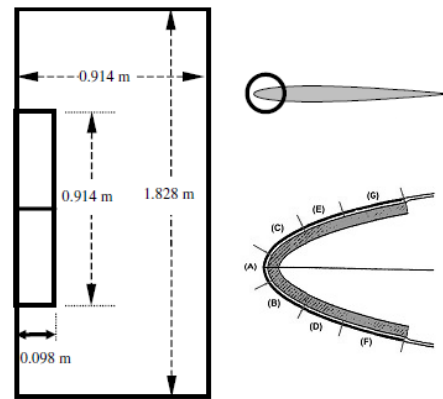


Fig.3 Structure and Size of the Test Component

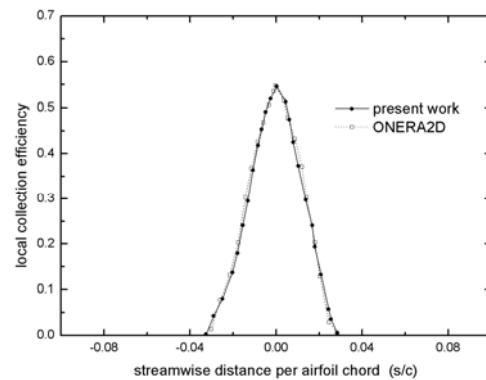


Fig.4 Local Collection Efficiency Calculation

Fig.5 shows the surface temperature results calculated by the program using experienced convection heat transfer coefficient. There is some difference between this result and experimental result in dry regions. It seems that in dry regions, the convection heat transfer

coefficient using experiential expressions may result in lower temperature on the surface.

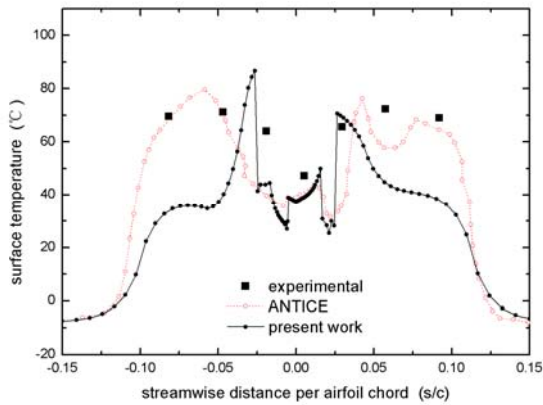


Fig.5 Surface Temperature Calculation

5.2 The effect of MVD in water droplet impingement

For different droplet mean volume diameters (MVD), the impingement characteristics are different. In this paper, the impingement characteristics of different MVDs are calculated. The results of local collection efficiency are shown in Fig.6 and the impinging trajectories are shown in Fig.7.

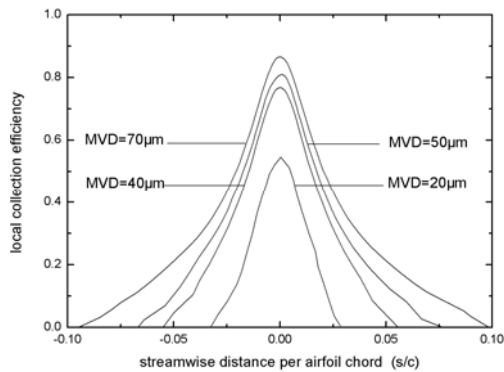
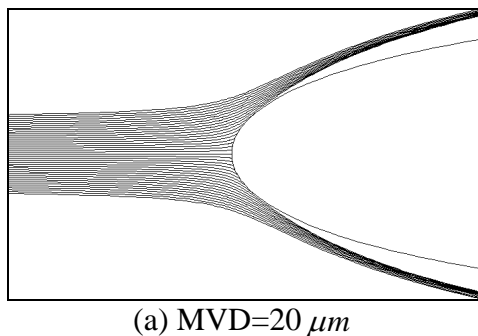
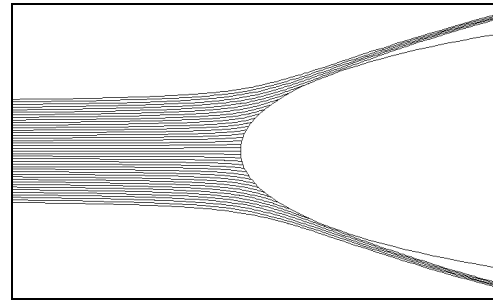


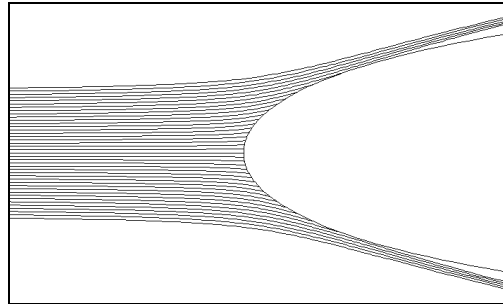
Fig.6 Local Collection Efficiency of Different MVDs



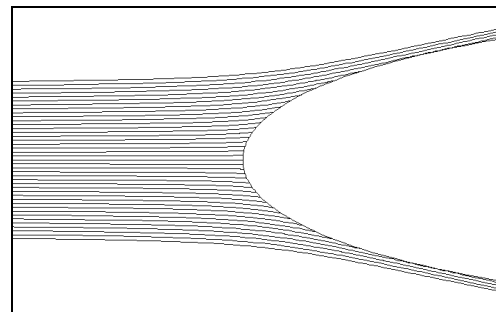
(a) MVD=20 μm



(b) MVD=40 μm



(c) MVD=50 μm



(d) MVD=70 μm

Fig.7 Water Droplet Impingement Trajectories of Different MVDs

The above pictures show that both the local collection efficiency and the impinging area increase when the droplet MVD increase. So when aircrafts pass through clouds which contain large water droplets, more anti-icing energy is needed.

5.3 The effect of heat transfer coefficient

The coefficient may influence the results of the temperature on the surface. The coefficients calculated by CFD are also given in this paper. The results are shown in Fig.8, and the surface temperature calculated using the heat transfer coefficient computed by CFD is shown in Fig.9. Obviously, the results using the coefficients which calculated by CFD are much closer to the

experimental data. The computation results show that heat transfer coefficient is one of the key parameters in the calculation of surface temperature.

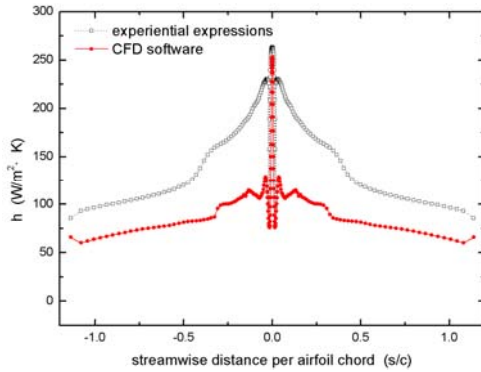


Fig.8 Comparison of Convection Heat Transfer Coefficient

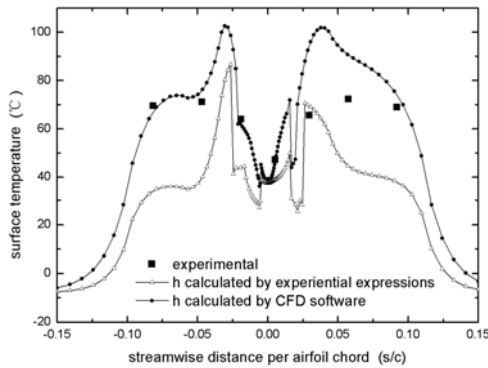


Fig.9 Comparison of Surface Temperature

5.4 The effect of LWC

LWC is another key parameter which can affect the surface temperature. In this paper the freestream condition of $LWC=0.9g/m^3$ is also calculated. The results of surface temperature distribution and mass flow rate of water film are shown in Fig.10 and Fig.11 comparing with $LWC=0.78g/m^3$.

Fig.10 and Fig.11 show that $LWC=0.78g/m^3$ and $LWC=0.9g/m^3$ don't affect the impingement region surface temperature seriously under this computation condition, because each kind of heat flux in this region doesn't change greatly as LWC changes. But in some other regions, higher LWC will result in lower surface temperature.

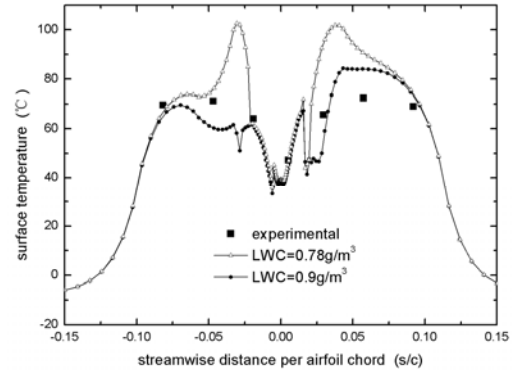


Fig.10 Surface Temperature with Different LWCs

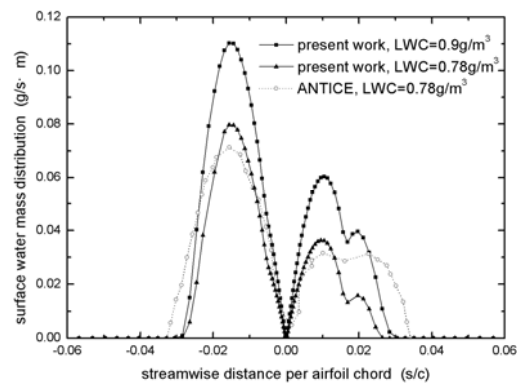


Fig.11 Surface Water Mass Flow Rate with Different LWCs

5.5 The effect of MVD

Large MVD will lead to the increase of the local collection efficiency and impinging area and decrease the surface temperature. The results of surface temperature using $MVD=20\ \mu m$ and $MVD=40\ \mu m$ at $LWC=0.78g/m^3$ are shown in Fig.12. Computation results show that the surface temperature decreases when the MVD increases.

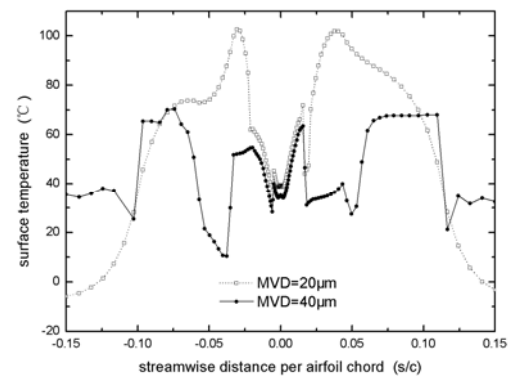


Fig.12. Surface Temperature with Different MVDs

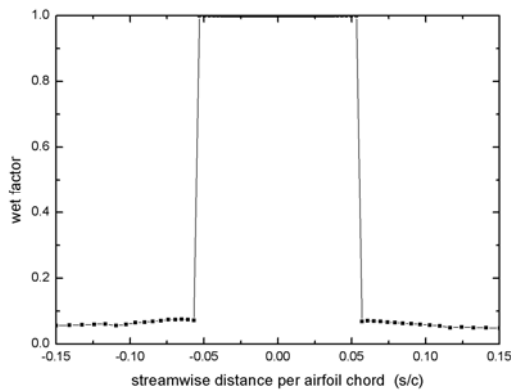


Fig.13. Wet Factor on the Surface MVD=40 μm

Fig.13 shows the wet factor on the surface when MVD=40 μm at LWC=0.78g/m³. Out of the impinging region, the wet factor is very small, which means the runback water mass flow rate is less than the critical mass flow rate. Under this condition, the runback flow should be rivulet flow.

Considering of the probable inaccuracy of the wet factor assuming unit in wet region, it is needed to do further research.

5.6 Analysis of different heat flux

It is necessary to find out the heat transfer process in anti-icing surface. The heat flux percentages of heating or cooling the surface are given, the results are shown in Fig.13 and Fig.14.

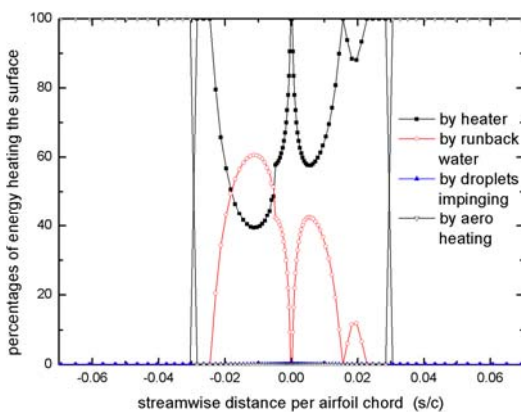


Fig.14 Heat Flux Percentages of Heating the Surface

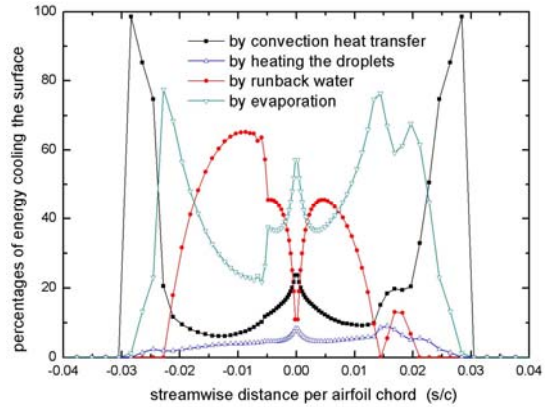


Fig.15 Heat Flux Percentages of Cooling the Surface.

Fig.14 shows that the heat flux of aero heating and water droplet impingement can be neglected. The water film on the surface can absorb some energy and bring the energy to downstream.

Fig.15 shows that the two largest heating flux terms are the water evaporating and convection heat transfer. The rest is mostly taken away by heating the water droplets. Runback water absorbs and stores the energy and takes it to downstream.

6 Conclusion

Based on the analysis of droplets movement equation and energy balance on the surface, an improved anti-icing model considering the coupling effects of water film layer and the air boundary layer is developed. A water film break-up analysis method using stability energy balance theory is introduced for calculating surface wetness factor distribution. Using the modified model, a special program is developed to calculate the surface temperature of the anti-icing wings, and the computation results are compared with the experiment results. Furthermore, the percentages of the different heat flux on the surface are analyzed and the effect factors on surface temperature in calculation are also given.

The results show that convection heat transfer coefficient is a very important parameter in surface temperature calculations. MVD of water droplets make a notable impact on surface temperature, because larger MVD

leads to larger local collection efficiency and impinging area.

The heat flux percentages of heating or cooling the surface show that the two largest heating flux terms are the water evaporating and convection heat transfer. In addition, the energy of heating impingement liquid water cannot be neglected.

Using the water film break-up model developed in this paper, the results of the wet factor is very small at out of the impinging region under the computation flow condition. Further research of this problem is needed.

References

- [1] Kind R J, Potapczuk M G, Feo A, Golia C, Shah A D. Experimental and computational simulation of in-flight icing phenomena. *Progress in Aerospace Science*. Vol.34, pp. 257-345, 1998.
- [2] Potapczuk M G. A review of NASA Lewis' development plans for computational simulation of aircraft icing. AIAA-99-0243, 1999
- [3] Tran P, Brahimi M T, Tezok F, Paraschivoiu I. Numerical simulation of ice accretion on multiple element configurations. AIAA 96-0869,1996
- [4] Hou Y ZH, Mechanism study on heat transfer and flow of hot air anti-icing for guide vane. M.S. Thesis, Shanghai Jiaotong Univ., Shanghai, 2009.
- [5] Bourgault Y, Habashi W G, Dompierre J, Boutanios Z, Di Bartolomeo W. An Eulerian approach to supercooled droplets impingement calculations. AIAA 97-0176, 1997.
- [6] Messinger B L. Equilibrium temperature of an unheated icing surface as a function of air speed. *Journal of the Aeronautical Sciences*, Vol.20, pp.29–42.1953.
- [7] Al-Khalil K M, Numerical simulation of an aircraft anti-icing system incorporating a rivulet model for the runback water. Ph.D Thesis, Univ. of Toledo, Toledo, OH,1991.
- [8] Al-Khalil K M, Keith T G, DeWitt K J, Nathman J K and Dietrich D A. Thermal analysis of engine anti-icing systems. *Journal of Propulsion and Power*. Vol.6,No.5, pp.628-634, 1990.
- [9] Al-Khalil K M, Keith T G, DeWitt K J. New concept in runback water modeling for anti-iced aircraft surfaces. *Journal of Aircraft*. Vol.30, No.1, pp.41-49, 1993.
- [10] Yi X. Numerical computation of aircraft icing and study on icing test scaling law. Ph.D Thesis, China Aerodynamics Research and Development Center Mianyang, 2007.
- [11] Silva G A L, Silvaes O M, Zerbini E J G J. Numerical Simulation of Airfoil Thermal Anti-Ice

Operation Part 1: Mathematical Modeling. *Journal of Aircraft*. Vol.44, No.2, pp.627-633, 2007.

- [12] Silva G A L, Silvaes O M, Zerbini E J G J. Numerical Simulation of Airfoil Thermal Anti-Ice Operation Part 2: Implementation and Results. *Journal of Aircraft*. Vol.44, No.2, pp.635-641, 2007.
- [13] Al-Khalil K M, Horvath C, Miller D R and Wright W. Validation of NASA Thermal Ice Protection Computer Codes Part 3:Validation of ANTICE. NASA TM 2001-210907, Cleveland, OH, May 2001.
- [14] Whalen E A, Broeren A P, Bragg M B. Aerodynamic of scaled runback ice accretions. *Journal of Aircraft*. Vol.45, No.2, pp.591-603, 2008.

Copyright Statement

The authors confirm that they hold copyright on all of the original material included in this paper. The authors also confirm that they have obtained permission, from the copyright holder of any third party material included in this paper, to publish it as part of their paper. The authors confirm that they give permission, or have obtained permission from the copyright holder of this paper, for the publication and distribution of this paper as part of the ICAS2010 proceedings or as individual off-prints from the proceedings.

Acknowledgements

The authors would like to recognize people who made this research program possible. The authors at Shanghai Jiaotong University were supported by the National Natural Science Foundation of China under Grant No.10772118